Inducible response required for repair of low-dose radiation damage in human fibroblasts

Saskia Grudzenski[a], Antonia Raths[a], Sandro Conrad[a], Claudia E. Rübe[b], and Markus Löbrich[a,1]

[a]Radiation Biology and DNA Repair, Darmstadt University of Technology, 64287 Darmstadt, Germany; and [b]Department of Radiation Oncology, Saarland University, 66421 Homburg/Saar, Germany

Edited* by Philip C. Hanawalt, Stanford University, Stanford, CA, and approved July 1, 2010 (received for review February 24, 2010)

Ionizing radiation (IR) induces a variety of DNA lesions among which DNA double-strand breaks (DSBs) are the biologically most significant. It is currently unclear if DSB repair is equally efficient after low and high doses. Here, we use γ-H2AX, phospho-ATM (pATM), and 53BP1 foci analysis to monitor DSB repair. We show, consistent with a previous study, that the kinetics of γ-H2AX and pATM foci loss in confluent primary human fibroblasts are substantially compromised after doses of 10 mGy and lower. Following 2.5 mGy, cells fail to show any foci loss. Strikingly, cells pretreated with 10 μM H_2O_2 efficiently remove all γ-H2AX foci induced by 10 mGy. At the concentration used, H_2O_2 produces single-strand breaks and base damages via the generation of oxygen radicals but no DSBs. Moreover, 10 μM H_2O_2 up-regulates a set of genes that is also up-regulated after high (200 mGy) but not after low (10 mGy) radiation doses. This suggests that low radical levels induce a response that is required for the repair of radiation-induced DSBs when the radiation damage is too low to cause the induction itself. To address the in vivo significance of this finding, we established γ-H2AX and 53BP1 foci analysis in various mouse tissues. Although mice irradiated with 100 mGy or 1 Gy show efficient γ-H2AX and 53BP1 foci removal during 24 h post-IR, barely any foci loss was observed after 10 mGy. Our data suggest that the cellular response to DSBs is substantially different for low vs. high radiation doses.

double-strand break repair | low radiation doses | inducible response

Ionizing radiation (IR) induces a variety of lesions of which DNA double-strand breaks (DSBs) are arguably the biologically most significant because unrepaired or misrepaired DSBs can lead to cell death and genomic instability (1, 2). The cell responds to the presence of DSBs with a sophisticated signal transduction pathway that orchestrates the repair process, initiates cell cycle checkpoint arrest, and induces apoptosis if necessary. In recent years, research has provided impressive mechanistic insight into the pathways governing the cellular response to IR; however, many of these studies have investigated the DNA damage response pathways under situations when a cell harbors an amount of lesions that is rarely encountered in nature during normal physiological processes.

The radiation doses that can potentially be encountered during a person's life range from a few milligray to several 10s of gray. The average lethal dose to a human cell is about 5 Gy, and if applied to the whole body, this dose can be lethal to a human being. Even higher doses are encountered during radiation therapy when tumor cells need to be inactivated. In contrast to these situations, radiodiagnostic investigations encompass much lower doses, with angiographic procedures and computer tomography scans representing high-dose radiodiagnostic examples in the dose range of several 10s of milligray (3–7). The most frequent radiodiagnostic examinations, x-ray scans, typically involve doses of less than 1 mGy. Also, the annual dose received from natural sources is on the order of a few milligray. Many people will never encounter high radiation doses during their life but will likely be exposed to doses in the milligray range. Thus, it is of outmost importance to estimate the risk (most importantly, the cancer risk) that is associated with low-dose exposures. Moreover, there is a need to investigate the efficiency of the damage response pathways and evaluate if and how the knowledge gained from experiments using high radiation doses can be applied to situations in which the cellular system is only marginally disturbed.

The risk estimates currently available are based primarily on epidemiological data from the atomic bomb survivors of Hiroshima and Nagasaki in Japan. These studies have provided risk estimates that increase linearly with dose for moderate to high doses (>50–100 mGy) (8, 9). Estimates below this level are difficult to obtain directly from epidemiological data. However, for practical regulatory purposes, it is assumed that linearity with dose also exists below this level. The validity of such a linear extrapolation from the moderate/high-dose range into the dose range of a few milligray would require that the biological processes involving the efficiency with which cells respond to the presence of DNA damage are equally efficient after low and high doses (10–13). However, several radiobiological phenomena, including the bystander effect, low-dose hypersensitivity, or delayed genomic instability, challenge the assumption of a linear dose–effect relationship, although most of these studies were performed with cells in culture after moderate to high doses (14, 15). Thus, their in vivo relevance in the milligray range is often unclear.

An important step during the cellular response to DSBs is the phosphorylation of the histone H2AX at the break site, giving rise to discrete nuclear foci, termed γ-H2AX foci (16). Subsequent to these phosphorylation events, several proteins, including 53BP1 and phospho-ATM (pATM), accumulate at the break sites and can also be visualized as distinct foci (17–19). We and others have shown that foci arise in a 1:1 relationship to DSBs and that the kinetics of foci loss reflect repair of DSBs (16, 20–22). This technology has the sensitivity that is necessary to investigate milligray doses and can be applied to various cell types and tissue samples (4, 5, 23–27).

Using primary human fibroblasts in culture in a previous study, we obtained the surprising finding that DSBs induced by low radiation doses (a few milligray) are repaired at a slower rate than DSBs produced by higher doses (25). Here, we show that primary human fibroblasts fail to repair DSBs induced by doses of 10 mGy efficiently but can repair the breaks if they are treated with 10 μM H_2O_2 before irradiation. H_2O_2 produces single-strand breaks (SSBs) and base damages via the generation of oxygen radicals but no DSBs at the concentration used. Strikingly, 10 μM H_2O_2 up-regulates a set of genes that is also up-regulated after high (200 mGy) but not after low (10 mGy) radiation doses. Thus, low levels of oxygen radicals induce a response that is required for the repair of radiation-induced DSBs when the radiation damage is too low to cause the induction by itself. Moreover, we irradiated mice with low to high radiation doses and show that DSBs, monitored by the presence of 53BP1 and γ-H2AX foci, persist in all analyzed tissues after low doses but not after moderate or high doses. The phe-

Author contributions: M.L. designed research; S.G., A.R., and S.C. performed research; C.E.R. contributed new reagents/analytic tools; S.G., A.R., S.C., and M.L. analyzed data; and M.L. wrote the paper.

The authors declare no conflict of interest.

*This Direct Submission article had a prearranged editor.

Freely available online through the PNAS open access option.

[1]To whom correspondence should be addressed. E-mail: lobrich@bio.tu-darmstadt.de.

This article contains supporting information online at www.pnas.org/lookup/suppl/doi:10.1073/pnas.1002213107/-/DCSupplemental.

CELL BIOLOGY

nomenon of inefficient DSB repair after milligray doses therefore also exists in vivo. Thus, the efficiency of arguably the most important damage response process after IR, the repair of DSBs, is clearly different in the milligray range compared with moderate and high radiation doses, challenging one of the most important assumptions for risk estimates in the low-dose range.

Results

Residual γ-H2AX Foci in Confluent Primary Human Fibroblasts After Low-Dose Exposure. A requirement for a reliable quantification of DSBs and their repair after low radiation doses is a low and highly reproducible DSB background level. Because DNA replication represents one source for spontaneous DSBs, we investigated cell cultures that can be maintained in confluency for prolonged periods of time. The primary human fibroblast line, HSF1, was grown to confluency for at least 3–4 weeks before analysis. The fraction of replicating cells, as assessed by BrdU incorporation, was less than 1% in such confluent cultures (Fig. S1). The level of spontaneous γ-H2AX foci varied between 0.08 and 0.17 foci per cell (Fig. 1 *A* and *B* and Fig. S2). We also used a second marker for DSBs, pATM, and obtained similar background levels (Fig. S3 *A* and *B*).

We have previously reported that the kinetics of γ-H2AX foci loss are strongly dependent on dose, with cells exposed to 200 mGy or higher showing much faster repair kinetics than cells irradiated with a few milligray of X-rays (25). Here, we investigated a range of doses between 2.5 and 200 mGy and show that the level of initial γ-H2AX and pATM foci at 5 min postirradiation depends linearly on dose, with a yield of ≈20 foci per 1 Gy per cell, similar to the yield obtained in previous studies with much higher doses (28) (Fig. 1*C* and Fig. S3*C*). Importantly, however, the rate of repair up to 24 h postirradiation was similar for 40, 80, and 200 mGy but significantly slower after 2.5, 10, and 20 mGy (Fig. 1*D*). At the lowest dose studied, 2.5 mGy, we did not observe any significant γ-H2AX foci loss for up to 72 h postirradiation. This finding was confirmed by the analysis of pATM foci, which provided repair kinetics similar to those of γ-H2AX foci (Fig. S3*D*).

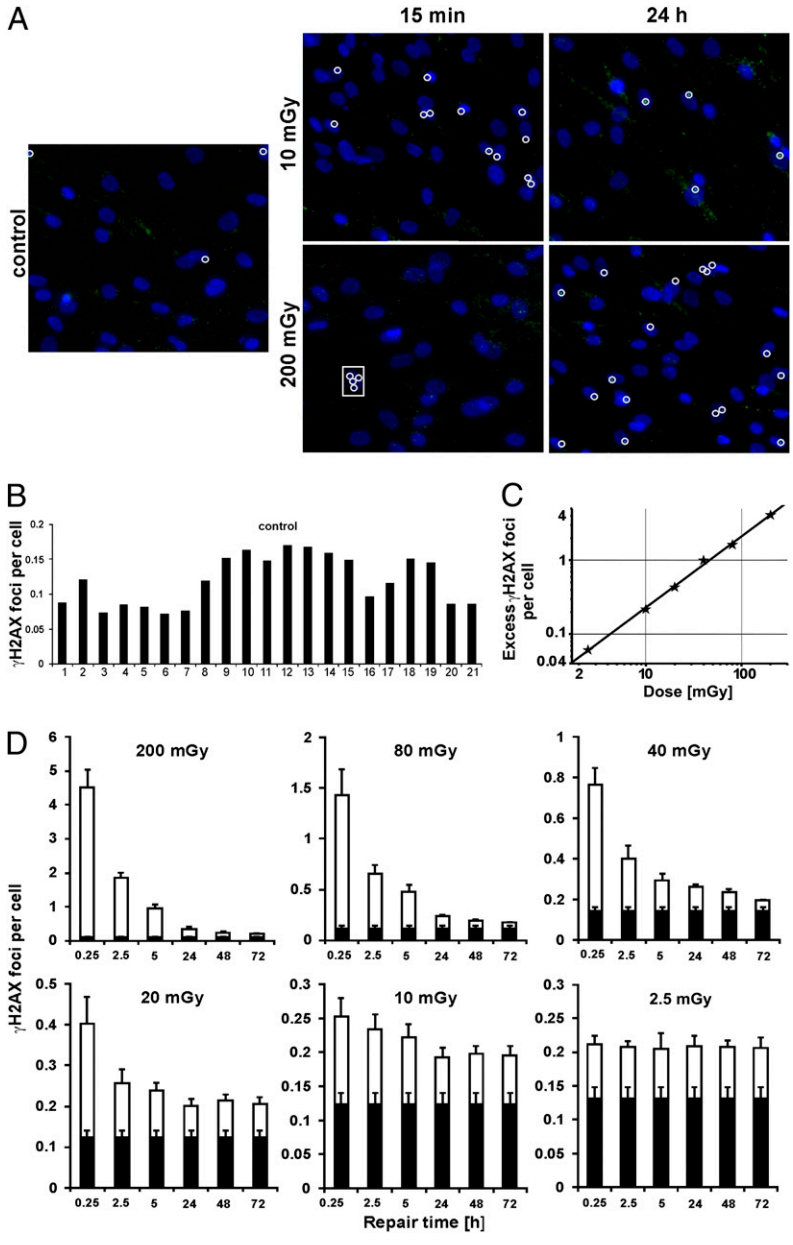

Fig. 1. Spontaneous γ-H2AX foci and kinetics for IR-induced γ-H2AX foci in the primary human fibroblast line, HSF1. (*A*) Representative images of γ-H2AX staining. Each white circle marks a γ-H2AX focus (green). Several foci are induced at 15 min after 200 mGy in each cell, but the foci are only marked in one cell (inside the rectangle). Enlarged versions of these images are shown in Fig. S2. (*B*) Background numbers of foci were assessed in 21 different samples from 10 independent experiments. (*C*) Foci numbers at 5 min postirradiation with 2.5–200 mGy. The line represents a linear fit to the data points (~21 foci per 1 Gy). (*D*) Kinetics for the loss of foci after different radiation doses. It can be seen that the efficiency of foci loss decreases with decreasing IR doses from 200 to 2.5 mGy. After 2.5 mGy, the number of induced foci per cell does not change for up to 72 h post-IR. Mean values from three different experiments are displayed. The black parts of the columns represent background values that were obtained from samples analyzed in the same experiment as the irradiated samples. In each experiment, at least one control sample was analyzed together with the six time points of a given dose. Error bars represent the SEM.

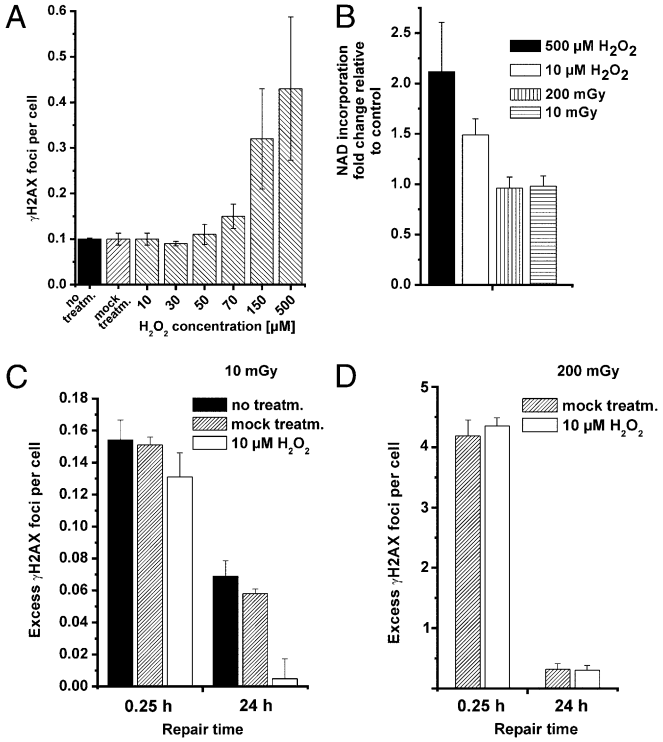

Fig. 2. γ-H2AX foci levels in the primary human fibroblast line HSF1 after H_2O_2 treatment alone or followed by irradiation. (*A*) γ-H2AX foci levels at 15 min after treatment (treatm.) with different concentrations of H_2O_2. The foci numbers of cells treated with concentrations up to 50 μM are similar to those of untreated and mock-treated cells. Higher concentrations of H_2O_2 lead to an increase in foci numbers. (*B*) PAR synthesis measured by nicotinamide-adenine dinucleotide incorporation at 15 min posttreatment with 10 or 500 μM H_2O_2 or with 10- or 200-mGy IR. γ-H2AX foci levels at 15 min and 24 h after 10 (*C*) or 200 (*D*) mGy. Cells were either untreated, mock-treated, or treated with 10 μM H_2O_2 before irradiation. Background foci numbers (~0.1 focus per cell) were subtracted in *C* and *D* but not in *A*. Error bars represent the SEM.

Pretreatment of Confluent Primary Human Fibroblasts with H_2O_2 Abolishes the Residual γ-H2AX Foci Level. The results above show that cells exhibit normal repair kinetics after doses that induce about one γ-H2AX focus per cell (40 and 80 mGy) but slower kinetics, or even a lack of repair, after lower doses, inducing a γ-H2AX focus in only a fraction of the analyzed cells. Thus, cells harboring a single γ-H2AX focus, which was induced by 40 or 80 mGy, appear to be able to repair this lesion but fail to repair a single γ-H2AX focus efficiently if it was induced by 2.5 or 10 mGy. This consideration led us to the idea that lesions other than DSBs, which are induced in sufficient quantity after 40 or 80 mGy but not after 2.5 or 10 mGy, might affect the efficiency of DSB repair. To test this idea, we used H_2O_2, which produces oxidative damage via the generation of hydroxyl radicals similar to IR. However, in contrast to IR, H_2O_2 produces many more SSBs and more base damage than DSBs. Indeed, the ratio of SSBs to DSBs is on the order of 20:1 for IR (29) but about 10,000:1 for H_2O_2 (30). Thus, by treating cells with H_2O_2, it is possible to induce high numbers of SSBs and base damage without any significant induction of DSBs.

We first investigated the induction of γ-H2AX foci for a range of H_2O_2 concentrations and observed that concentrations of 50 μM and below do not measurably affect the γ-H2AX background level in confluent HSF1 cells, whereas 150 and 500 μM H_2O_2 lead to a significant induction of γ-H2AX foci (Fig. 2*A*). For further experiments, we used a concentration of 10 μM, which does not induce any γ-H2AX foci but is expected to produce multiple SSBs and base damages (31). Consistent with this, the level of SSBs measured by poly-(ADP)-ribose (PAR) synthesis was significantly elevated following H_2O_2 treatment with 10 μM (Fig. 2*B*). Strikingly, cells pretreated with 10 μM H_2O_2 showed the same level of γ-H2AX foci induction by a dose of 10 mGy as untreated cells but, in contrast to untreated cells, were able to repair all IR-induced γ-H2AX foci within 24 h (Fig. 2*C*). Lower concentrations of H_2O_2 were less efficient to "activate" repair after 10 mGy (Fig. S4), and 10 μM H_2O_2 did not affect foci levels after 200 mGy (Fig. 2*D*). Thus, the oxidative damage induced by H_2O_2 treatment did significantly affect the repair efficiency of DSBs induced by low doses of IR.

Gene Expression After H_2O_2 Treatment or Irradiation. The results above suggest that 10 μM H_2O_2 induces a response that is needed for the repair of DSBs after low but not after high radiation doses. To test this, we performed gene expression experiments using highly confluent HSF1 cells. We treated the cells with 10 μM H_2O_2 or irradiated them with 10 or 200 mGy and assessed mRNA levels at 5 h posttreatment. We observed that from a total of about 33,000 genes analyzed in four experiments, 24 genes were significantly up-regulated after a dose of 200 mGy relative to untreated cells (1 gene was significantly down-regulated). After 10 μM H_2O_2, 18 genes were up-regulated, and after 10 mGy IR, 7 genes were up-regulated (Table S1). Strikingly, 6 of the 24 genes up-regulated after 200 mGy were also up-regulated after 10 μM H_2O_2 but not after 10 mGy (1 gene was up-regulated after all three treatment conditions) (Table 1). At least 1 of the 6 genes appears to be involved in the IR-induced DNA damage response (32, 33).

γ-H2AX Foci in Mouse Tissue After Low-Dose Exposure. We have previously used γ-H2AX foci analysis to study the induction and repair of DSBs in various mouse tissues after high radiation doses (34). Here, we irradiated C57BL/6 mice with doses of 10 mGy, 100 mGy, or 1 Gy and removed organs at defined time points after irradiation. Tissue samples of the heart, small intestine, and kidney were stained against 53BP1 or γ-H2AX, and foci were enumerated (Fig. 3*A* and Figs. S5 and S6). All samples analyzed after 10 mGy (three different tissues from three different mice) showed 53BP1 foci levels higher than control samples (three different tissues from nine different mice), with about 0.08 induced foci at 10 min post-IR for all three tissues (Fig. 3*B*). Following doses of 100 mGy and 1 Gy, we also observed a similar number of 53BP1 foci in the three investigated tissues (about 0.6 and 7 foci per cell at 10 min after 100 mGy or 1 Gy, respectively) (Fig. 3*C*). Thus, foci induction is similar in various mouse tissues and increases linearly with dose from 10 mGy to 1 Gy. The induction yield of about 7 foci per cell

Table 1. List of genes that are significantly up-regulated in confluent primary human fibroblasts after 200-mGy IR and 10 μM H_2O_2 but not after 10-mGy IR

Public identification no.	Gene title	Gene symbol
AI927479	Hypothetical protein LOC552889	*LOC552889*
AI739378	Euchromatic histone-lysine *N*-methyltransferase 1	*EHMT1*
AI768512	WNK lysine-deficient protein kinase 1	*WNK1*
Z25431	NIMA (never in mitosis gene a)-related kinase 1	*NEK1*
AI049791	Biorientation of chromosomes in cell division 1-like	*BOD1L*
NM_007211	Ras association (RalGDS/AF-6) domain family	*RASSF8*

CELL BIOLOGY

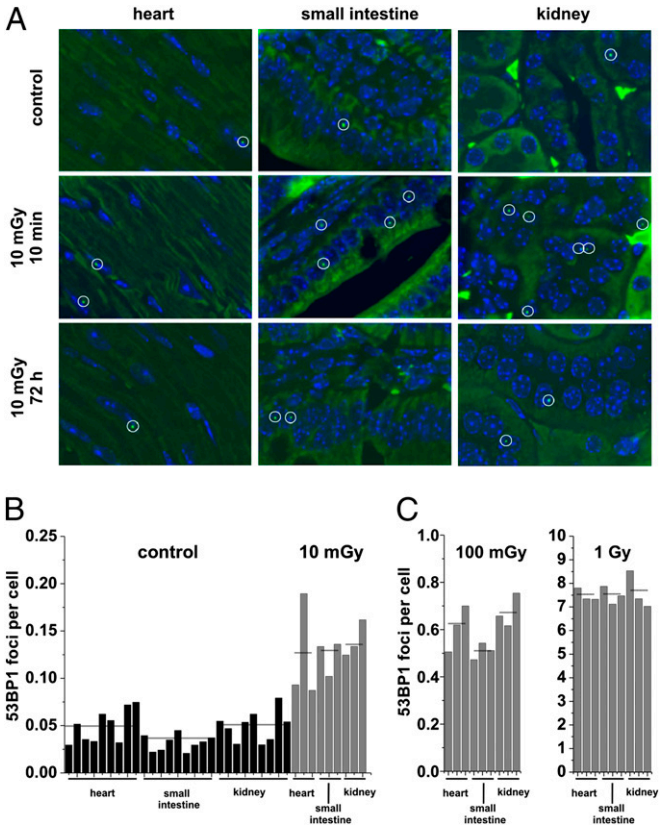

Fig. 3. Spontaneous and IR-induced 53BP1 foci in various mouse tissues. (*A*) Representative images of 53BP1 staining (green) in the heart, small intestine, and kidney of unirradiated or irradiated C57BL/6 mice analyzed at 10 min or 72 h after in vivo irradiation with 10 mGy. Enlarged versions of representative images after 10 mGy are shown in Fig. S5. Representative images after 1 Gy are shown in Fig. S6. (*B*) Foci levels were assessed in nine unirradiated mice and three mice analyzed at 10 min after 10 mGy. (*C*) Foci levels were assessed in three mice analyzed at 10 min after 100 mGy and three mice analyzed at 10 min after 1 Gy. All analyzed organs show the same linear dose correlation from 10 mGy to 1 Gy.

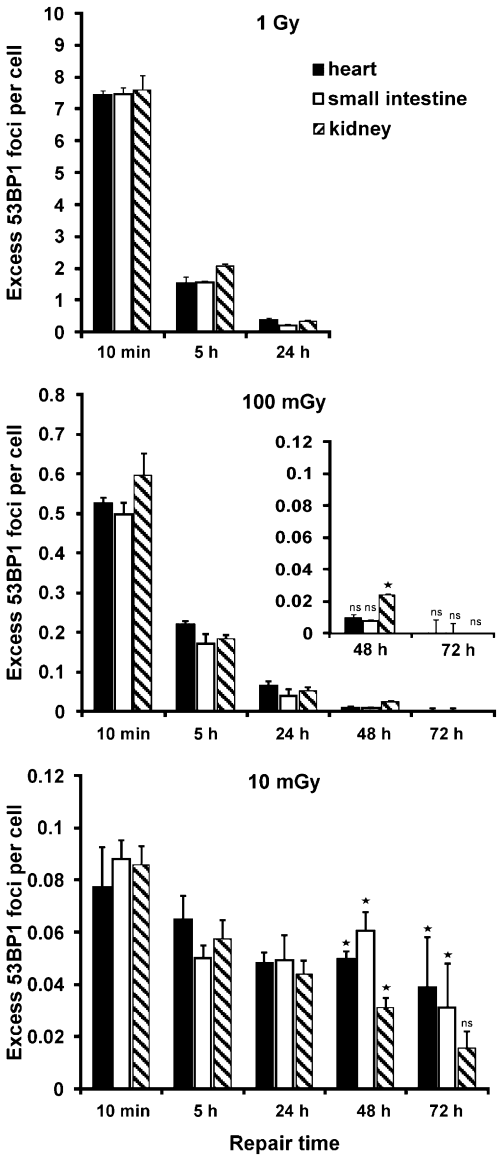

Fig. 4. Repair kinetics for IR-induced 53BP1 foci in the heart, small intestine, and kidney of C57BL/6 mice. Foci levels were analyzed up to 72 h after in vivo irradiation with 10 mGy, 100 mGy, or 1 Gy. All analyzed organs show similar foci levels. Efficient repair is observed after 100 mGy and 1 Gy but not after 10 mGy. Mean values from two to three mice are displayed. For samples with low foci numbers, several thousand cells per data point were analyzed. Background focus numbers were subtracted. Statistical analysis (one-tailed Student's *t* test) was performed for the 48- and 72-h data. The asterisk indicates significantly elevated foci levels compared with control samples ($P < 0.05$); ns, not significant. Error bars represent the SEM.

per 1 Gy at 10 min post-IR is similar to that of our previous study (34) but substantially lower than the level of 15–20 foci per 1 Gy typically observed for human cells in culture (28). We have previously suggested that this difference may reflect that mouse cells have a 20% lower DNA content than human cells, that additional foci loss can occur during the time necessary to retrieve and fix the organs, and that foci scoring in a cross-section of cells embedded in a tissue sample will significantly underestimate the true foci numbers (34). The results for γ-H2AX foci were slightly more variable than for 53BP1 foci but confirmed our finding that foci in tissues are induced linearly with a dose between 10 mGy and 1 Gy (about 0.07, 0.6, and 8 γ-H2AX foci per cell at 10 min after 10 mGy, 100 mGy, or 1 Gy, respectively) (Fig. S7).

Persistent γ-H2AX Foci in Low-Dose–Irradiated Mice. The low and reproducible background of 53BP1 and γ-H2AX foci in various mouse tissues offered the intriguing possibility to investigate DSB repair at low vs. high doses under in vivo situations. Following 1-Gy irradiation, 53BP1 foci were lost in all three tissues with kinetics similar to those in primary human fibroblasts in culture, with about 20–30% unrepaired foci after 5 h and less than 5% unrepaired foci after 24 h post-IR (Fig. 4). Efficient repair was also observed after a dose of 100 mGy; however, strikingly, foci were lost much less efficiently following a 10-mGy dose. In contrast to 5% unrepaired foci at 24 h after 100 mGy or 1 Gy, more than 50% of the initially induced 53BP1 foci persisted for up to 24 h after 10 mGy (Fig. 4). A nearly identical result was obtained from the analysis of γ-H2AX foci (Fig. S8). We also investigated repair times up to 3 d after 10 and 100 mGy. At 48 and 72 h, most tissues of mice irradiated with 10 mGy but not of mice irradiated with 100 mGy displayed higher 53BP1 foci levels than unirradiated tissues (Fig. 4 and Fig. S5).

Discussion

We have previously provided evidence that DSBs induced by radiation doses of a few milligray are repaired at a slower rate than DSBs produced by the higher doses typically used for analysis. In the present study, we confirm this finding and report on two significant advances. First, we show that pretreating cells with 10 μM H_2O_2, a concentration that does not measurably af-

fect the DSB background level but generates SSBs and base damage, improves the ability of these cells to repair DSBs induced by low radiation doses. This finding provides mechanistic insight into the phenomenon underlying the inefficient repair observed after low radiation doses. Second, and, arguably, equally important, we report that mice irradiated with low radiation doses fail to repair the IR-induced DSBs efficiently, demonstrating that the phenomenon is of relevance for the in vivo situation. Moreover, because inefficient repair is observed in three different tissues, it likely represents a general cellular phenomenon.

Our data show that cells are able to repair a single DSB efficiently if this break was induced by a dose of 40–80 mGy but fail to repair a single break that was induced by a dose of 10 mGy or lower. Thus, it is not the level of initial DSBs that determines whether repair is efficient or inefficient. We can think of at least two different models that can potentially explain this apparently unexpected finding. First, it could be possible that the level of DSBs in the neighboring cells affects the efficiency of repair [i.e., a cell may not repair its break when the neighboring cells are devoid of any DSBs (which is the case after 10 mGy and below) but may show efficient repair if all cells of a population harbor a break (at 40–80 mGy and above)]. Such an explanation would require an intercellular communication or bystander mechanism, which has been reported for cells and tissues (35). However, to date, we have no solid evidence that a bystander-like mechanism underlies the inefficient repair at low doses. Second, a cell may repair a single DSB after 40–80 mGy and above but not after 10 mGy and below because the lower doses produce a damage or stress level that is insufficient to allow for efficient DSB repair. According to this explanation, it is the level of radiation damage other than DSBs or some unknown cellular lesion arising from radiation damage that determines whether or not efficient DSB repair occurs. Our finding that cells are able to repair DSBs induced by 10 mGy efficiently if they were treated with 10 μM H_2O_2 before irradiation argues in favor of this second explanation. H_2O_2 is an agent producing oxidative damage similar to radiation. However, although radiation produces a ratio of SSBs to DSBs of about 20:1 (29), the SSB-to-DSB ratio after H_2O_2 treatment is on the order of 10,000:1 (30). We have recently reported that 25 μM H_2O_2 generates no detectable DSBs but a level of SSBs similar to several gray of x-rays (31). Here, we confirm that a measurable amount of DSBs only arises at H_2O_2 concentrations of 150 μM and above, whereas a significant level of SSBs, measured by PAR synthesis, is already produced by 10 μM H_2O_2. Thus, 10 μM H_2O_2 produces no measureable DSBs but generates a significant amount of oxidative lesions, including SSBs and base damage. It is possible that cells pretreated with 10 μM H_2O_2 show efficient DSB repair, even at low doses, because this treatment generates a level of SSBs or base damage that is necessary for inducing DSB repair and is insufficiently produced by low radiation doses.

In support of this model, we have observed that treatment with 10 μM H_2O_2 up-regulates a set of six genes that is also up-regulated by 200 mGy but not by 10 mGy. Strikingly, at least one of the six genes (Nek1) appears to be involved in DNA damage responses following IR, and its loss is associated with radiosensitivity and impaired DSB repair (32, 33). This finding is in line with other recent observations indicating that oxidative stress on proteins can modify their structure and function (36–39).

However, the question arises of how DSB repair might be linked to the repair of SSBs or base damage. One possible explanation is that radiation-induced DSBs have end structures that need processing before ligation (basically none of the DSBs induced by IR can be ligated without processing), and it is possible that such end-processing involves factors that are also involved in the response to SSBs or base damage and need to be induced. In any case, the data suggest that low levels of oxygen radicals induce a response that is needed for the repair of IR-induced DSBs when the radiation damage is too low to cause the response by itself. An inducible response has hitherto been shown for other DNA damage, including base damage, but not for DSBs. Clearly, this phenomenon needs to be investigated in more detail.

Our finding that cells are able to repair DSBs efficiently at low doses if exposed to oxidative stress before irradiation may also explain a recent study by Asaithamby and Chen (23). These authors used an elegant live cell imaging approach with cells transfected with YFP-tagged 53BP1 and reported that DSB repair after 5 mGy is as efficient as for higher doses (up to 1,000 mGy). It is possible that the experimental setup, including the visualization of foci in living cells using laser light, might generate an oxidative stress level that can affect the efficiency of repair after low radiation doses.

γ-H2AX foci analysis provides an exceptionally sensitive tool to study DSB repair processes at low radiation doses. We have used this technology in the past and at present to provide mechanistic insight into DSB repair pathways (40, 41). We have provided ample evidence that after irradiation of nonreplicating cells, γ-H2AX foci represent DSBs and that the kinetics of foci loss represent DSB repair (31). However, all these studies were performed at doses on the order of a few gray or at least several hundred milligray, when normal cells are able to repair DSBs efficiently. In the present study and in our previous work using low doses, we were unable to confirm our findings with alternative methods because none of the existing methods to study repair of DNA or chromosomal damage has the necessary sensitivity. Moreover, the phosphorylation of H2AX on DSB induction and, more relevant in this context, the dephosphorylation of γ-H2AX after repair represent highly complicated processes involving many enzymatic steps, highly orchestrated signaling pathways, and chromatin remodeling mechanisms. Thus, failure to remove γ-H2AX foci efficiently may represent a failure to repair DSBs; however, perhaps equally likely, it may reflect the inability to perform one of the many molecular steps required to dephosphorylate a γ-H2AX focus properly after DSB repair is complete. Notwithstanding this limitation, the available evidence suggests that a γ-H2AX focus represents a signal for an unrepaired DSB. Therefore, a cell will respond to this signal irrespective of whether the DSB is indeed unrepaired or whether it was repaired but simply not dephosphorylated. Differences in the rate of foci loss at low vs. high doses will therefore cause differences in the cellular response to low vs. high doses.

Several findings prompted us to investigate whether the observed in vitro differences in the efficiency of DSB repair for low vs. high doses have relevance for the in vivo situation. First, the observation that slight changes in the oxidative stress level can have an impact on the efficiency of DSB repair suggests that results of in vitro studies may depend on the specific cell culture conditions. Second, differences in the efficiency of DSB repair for low vs. high doses were not observed in cells analyzed by live cell imaging (23). Third, most cell lines in culture exhibit high background foci levels, which make it difficult to analyze DSB repair after low doses in vitro (26). Thus, we refined our previously published methodological approach to investigate DSB repair after low radiation doses in various tissues of irradiated mice (34). Using the analysis of 53BP1 and γ-H2AX foci in tissue sections of the heart, small intestine, and kidney, we were able to show that mice that underwent whole-body irradiation with 10 mGy fail to repair DSBs efficiently. Even at 24 h postirradiation, tissue samples from 10-mGy–irradiated mice could easily be distinguished from tissue samples of unirradiated mice (Fig. S5). This finding offers the intriguing possibility that low-level exposures can be identified retrospectively after prolonged times in biological samples. Indeed, we observed persisting 53BP1 foci for up to 3 d after 10-mGy irradiation.

In conclusion, we present evidence that an inducible response is required for efficient repair of DSBs in human fibroblasts. We suggest that this response is initiated after high doses by the radiation itself. After low doses, however, the radiation dose is insufficient to induce this response and DSB repair is inefficient. The response can then be induced by pretreatment with H_2O_2, which produces oxidative radicals similar to radiation but no DSBs at the concentration used. Finally, we demonstrate that

irradiated mice also show inefficient DSB repair after low radiation doses, providing in vivo evidence for this phenomenon.

Materials and Methods

Experiments with H_2O_2. HSF1 cells were covered with ice-cold PBS containing H_2O_2 and incubated at 4 °C for 30 min. Mock-treated cells were handled the same way, but the PBS did not contain H_2O_2. Cells were then washed twice with PBS at room temperature and kept in cell culture medium at 37 °C for 15 min. Cells were then fixed to assess foci formation attributable to H_2O_2 treatment. For irradiation experiments, samples were treated with H_2O_2 or mock-treated and then immediately irradiated and fixed 15 min or 24 h postirradiation.

Irradiation of HSF1 Cells. Irradiation was performed with an x-ray machine (PW2184; Philips) at 90 kV, 6 mA, and a dose rate of 70 mGy/min, determined with a dosimeter (PTW-SN4, type 7612; PTW) and chemical dosimetry. We have considered in the present study that cells irradiated on glass slides receive a dose that is higher, as determined by physical and chemical dosimetry (28).

Animal Irradiation (in Vivo) and Tissue Isolation. Adult C57BL/6 (C57BL/6NCrl) mice (Charles River Laboratories) received whole-body irradiation using a linear accelerator (6-MV photons). The dose rate, as determined by a physical dosimeter, was 2 Gy/min for 100-mGy and 1-Gy doses (source-skin distance about 1 m) or about 0.35 Gy/min for the 10-mGy dose (source-skin distance about 2.5 m). All mice were irradiated in a special cylinder consisting of a tissue-equivalent plastic material (1.5-cm thickness) providing uniform dose deposition throughout the whole body of each individual mouse. The irradiation setup was evaluated by means of an ADAC Pinnacle 3D treatment planning system (ADAC Laboratories). Mice were anesthetized directly before the end of repair time. Subsequently, the heart, kidney, and small intestine were removed and placed in 4% (vol/vol) neutral buffered formalin for 16 h. Formalin-fixed tissues were embedded in paraffin and sectioned at a thickness of 4 μm. The animal studies were approved by the Medical Sciences Animal Care and Use Committee of the University of Saarland.

γ-H2AX and 53BP1 Immunofluorescence of Tissues and Fibroblasts. After dewaxing in xylene and rehydration, sections were incubated in citrate buffer for 1 h at 95 °C and incubated with PBS with 1% goat serum (Biochrom) for 1 h at room temperature. Sections were incubated with anti-γ-H2AX antibody (Upstate) at a ratio of 1:800 or with anti-53BP1 antibody (Rockland Laboratories) at a ratio of 1:600 overnight at 4 °C, washed three times for 10 min each time in PBS, incubated with goat-anti-mouse or goat-anti-rabbit antibody (Alexa Fluor 488 and 594, respectively; Invitrogen) at a ratio of 1:200 for 1 h at room temperature, washed four time for 10 min each time, and mounted in VECTASHIELD mounting medium (Vector Laboratories) with DAPI. Fibroblasts were analyzed as described elsewhere (21).

Foci Analysis. In the heart, the myocardium of ventricles, consisting of striated fibers, was used for foci analysis; only cells with longitudinally cut nuclei were scored. Foci analysis in the small intestine was confined to the nondividing epithelial cells of the villi of the mucosal surface. Foci analysis in the kidney was in the renal cortex, with cells of the glomeruli and proximal and distal convoluted tubules.

Foci counting by eye was typically performed in a blinded manner. Fluorescence images were captured using Axiovision 40 V 4.6.3-SP1-Software (Zeiss) or METAFER 4 V3.4.0 Software (Meta Systems) at a magnification of 630×. All images are maximum intensity projections of image stacks ($z = 40$) with focus plane distances of 300 nm. The images in Fig. 3A and Fig. S5 were deconvolved using Huygens 3.3.2p1 64b-Software (Scientific Volume Imaging). The images in Fig. 1*A* and Figs. S2, S3*A*, and S5 consist of several (4–9) single images assembled using Corel DRAW Graphics Suite ×3 (Corel Corporation).

PAR synthesis and gene expression analysis are described in *SI Materials and Methods*.

ACKNOWLEDGMENTS. We thank Penny Jeggo for insightful comments on this work and the manuscript, Eik Schumann for help with tissue imaging, and Alexander Rapp for help with the nicotinamide-adenine dinucleotide assay. The laboratory of M.L. is supported by the Deutsche Forschungsgemeinschaft (Grant Lo 677/4-1/2), Bundesministerium für Bildung und Forschung via Forschungszentrum Karlsruhe (Grants 02S8335 and 02S8355), and Forschungszentrum Jülich (Grant 03NUK001C).

1. Löbrich M, Jeggo PA (2007) The impact of a negligent G2/M checkpoint on genomic instability and cancer induction. *Nat Rev Cancer* 7:861–869.
2. van Gent DC, Hoeijmakers JH, Kanaar R (2001) Chromosomal stability and the DNA double-stranded break connection. *Nat Rev Genet* 2:196–206.
3. Brenner DJ, Elliston CD (2004) Estimated radiation risks potentially associated with full-body CT screening. *Radiology* 232:735–738.
4. Grudzenski S, Kuefner MA, Heckmann MB, Uder M, Löbrich M (2009) Contrast medium-enhanced radiation damage caused by CT examinations. *Radiology* 253:706–714.
5. Kuefner MA, et al. (2009) DNA double-strand breaks and their repair in blood lymphocytes of patients undergoing angiographic procedures. *Invest Radiol* 44:440–446.
6. Rothkamm K, Balroop S, Shekhdar J, Fernie P, Goh V (2007) Leukocyte DNA damage after multi-detector row CT: A quantitative biomarker of low-level radiation exposure. *Radiology* 242:244–251.
7. Brenner DJ, Hall EJ (2007) Computed tomography—An increasing source of radiation exposure. *N Engl J Med* 357:2277–2284.
8. Preston DL, et al. (2004) Effect of recent changes in atomic bomb survivor dosimetry on cancer mortality risk estimates. *Radiat Res* 162:377–389.
9. Pierce DA, Preston DL (2000) Radiation-related cancer risks at low doses among atomic bomb survivors. *Radiat Res* 154:178–186.
10. Brenner DJ, et al. (2003) Cancer risks attributable to low doses of ionizing radiation: Assessing what we really know. *Proc Natl Acad Sci USA* 100:13761–13766.
11. Goodhead DT (2009) Understanding and characterisation of the risks to human health from exposure to low levels of radiation. *Radiat Prot Dosimetry* 137:109–117.
12. Goodhead DT (2010) New radiobiological, radiation risk and radiation protection paradigms. *Mutat Res* 687:13–16.
13. Brenner DJ (2009) Extrapolating radiation-induced cancer risks from low doses to very low doses. *Health Phys* 97:505–509.
14. Averbeck D (2009) Does scientific evidence support a change from the LNT model for low-dose radiation risk extrapolation? *Health Phys* 97:493–504.
15. Tubiana M, Arengo A, Averbeck D, Masse R (2007) Low-dose risk assessment. *Radiat Res* 167:742–744, author reply 744.
16. Rogakou EP, Boon C, Redon C, Bonner WM (1999) Megabase chromatin domains involved in DNA double-strand breaks in vivo. *J Cell Biol* 146:905–916.
17. Schultz LB, Chehab NH, Malikzay A, Halazonetis TD (2000) p53 binding protein 1 (53BP1) is an early participant in the cellular response to DNA double-strand breaks. *J Cell Biol* 151:1381–1390.
18. Bekker-Jensen S, et al. (2006) Spatial organization of the mammalian genome surveillance machinery in response to DNA strand breaks. *J Cell Biol* 173:195–206.
19. So S, Davis AJ, Chen DJ (2009) Autophosphorylation at serine 1981 stabilizes ATM at DNA damage sites. *J Cell Biol* 187:977–990.
20. Kühne M, et al. (2004) A double-strand break repair defect in ATM-deficient cells contributes to radiosensitivity. *Cancer Res* 64:500–508.
21. Riballo E, et al. (2004) A pathway of double-strand break rejoining dependent upon ATM, Artemis, and proteins locating to gamma-H2AX foci. *Mol Cell* 16:715–724.
22. Sedelnikova OA, Rogakou EP, Panyutin IG, Bonner WM (2002) Quantitative detection of (125)IdU-induced DNA double-strand breaks with gamma-H2AX antibody. *Radiat Res* 158:486–492.
23. Asaithamby A, Chen DJ (2009) Cellular responses to DNA double-strand breaks after low-dose gamma-irradiation. *Nucleic Acids Res* 37:3912–3923.
24. Löbrich M, et al. (2005) In vivo formation and repair of DNA double-strand breaks after computed tomography examinations. *Proc Natl Acad Sci USA* 102:8984–8989.
25. Rothkamm K, Löbrich M (2003) Evidence for a lack of DNA double-strand break repair in human cells exposed to very low x-ray doses. *Proc Natl Acad Sci USA* 100:5057–5062.
26. Wilson PF, et al. (2010) Inter-individual variation in DNA double-strand break repair in human fibroblasts before and after exposure to low doses of ionizing radiation. *Mutat Res* 683:91–97.
27. Bonner WM, et al. (2008) GammaH2AX and cancer. *Nat Rev Cancer* 8:957–967.
28. Kegel P, Riballo E, Kühne M, Jeggo PA, Löbrich M (2007) X-irradiation of cells on glass slides has a dose doubling impact. *DNA Repair (Amst)* 6:1692–1697.
29. Nikjoo H, et al. (2002) Modelling of DNA damage induced by energetic electrons (100 eV to 100 keV). *Radiat Prot Dosimetry* 99:77–80.
30. Bradley MO, Kohn KW (1979) X-ray induced DNA double strand break production and repair in mammalian cells as measured by neutral filter elution. *Nucleic Acids Res* 7:793–804.
31. Löbrich M, et al. (2010) gammaH2AX foci analysis for monitoring DNA double-strand break repair: Strengths, limitations and optimization. *Cell Cycle* 9:662–669.
32. Chen Y, Chen PL, Chen CF, Jiang X, Riley DJ (2008) Never-in-mitosis related kinase 1 functions in DNA damage response and checkpoint control. *Cell Cycle* 7:3194–3201.
33. Polci R, Peng A, Chen PL, Riley DJ, Chen Y (2004) NIMA-related protein kinase 1 is involved early in the ionizing radiation-induced DNA damage response. *Cancer Res* 64:8800–8803.
34. Rübe CE, et al. (2008) DNA double-strand break repair of blood lymphocytes and normal tissues analysed in a preclinical mouse model: Implications for radiosensitivity testing. *Clin Cancer Res* 14:6546–6555.
35. Belyakov OV, et al. (2005) Biological effects in unirradiated human tissue induced by radiation damage up to 1 mm away. *Proc Natl Acad Sci USA* 102:14203–14208.
36. Bakkenist CJ, Kastan MB (2004) Initiating cellular stress responses. *Cell* 118:9–17.
37. Bravard A, et al. (2009) Oxidation status of human OGG1-S326C polymorphic variant determines cellular DNA repair capacity. *Cancer Res* 69:3642–3649.
38. Kensler TW, Wakabayashi N, Biswal S (2007) Cell survival responses to environmental stresses via the Keap1-Nrf2-ARE pathway. *Annu Rev Pharmacol Toxicol* 47:89–116.
39. Kensler TW, Wakabayashi N (2010) Nrf2: Friend or foe for chemoprevention? *Carcinogenesis* 31:90–99.
40. Beucher A, et al. (2009) ATM and Artemis promote homologous recombination of radiation-induced DNA double-strand breaks in G2. *EMBO J* 28:3413–3427.
41. Deckbar D, et al. (2007) Chromosome breakage after G2 checkpoint release. *J Cell Biol* 176:749–755.